



# Efficient recovery of rare earth elements from discarded NdFeB magnets by mechanical activation coupled with acid leaching

Fulin Mao<sup>1</sup> · Nengwu Zhu<sup>1,2,3,4</sup> · Wen Zhu<sup>1</sup> · Bowen Liu<sup>1</sup> · Pingxiao Wu<sup>1,2,3,4</sup> · Zhi Dang<sup>1,2,3</sup>

Received: 11 June 2021 / Accepted: 22 November 2021 / Published online: 29 November 2021  
© The Author(s), under exclusive licence to Springer-Verlag GmbH Germany, part of Springer Nature 2021

## Abstract

Due to the increasing demands and supply shortages for rare earth elements (REEs), the recovery of REEs from discarded NdFeB with high REE content has become extremely important. In this paper, a hydrometallurgical coupling process involving mechanical activation and selective acid leaching was proposed for the recovery of REEs from discarded NdFeB magnets. The effects of ball milling activation speed, hydrochloric acid concentration, and solid–liquid ratio on the leaching efficiencies of REEs in NdFeB magnets were studied. The results indicated that the ball milling activation method could enhance the reactivity of the samples through the action of mechanical force, which promoted the leaching efficiency and leaching speed of REEs. Under the optimum conditions (650-rpm activation speed, 0.4 M hydrochloric acid, 100 g/L solid–liquid ratio), the leaching efficiency of REEs increased up to 99% with low hydrochloric acid consumption and the leaching speed of REEs was triple than that of without activation. The final purity of recovered rare earth oxides reached up to 99.9%. All results demonstrated that ball milling activation coupled with selective leaching of hydrochloric acid could be an effective and environment-friendly strategy to achieve the recovery of REEs.

**Keywords** Rare earth elements · Discarded NdFeB magnets · Mechanical activation · Leaching

## Introduction

Rare earth elements (REEs) are a kind of very important metal elements, which are composed of scandium, yttrium, and fifteen kinds of lanthanide elements. Due to their excellent performances, they have been widely used in various high-tech products, especially in clean products such as

new energy vehicles, high-power fans, frequency conversion compressors, and energy-saving motors (Yang et al. 2017; Firdaus et al. 2018). With the continuous breakthrough of technology, the demand for REEs is expected to significantly increased in the near future. Meanwhile, many countries were facing supply risks due to the limited REE reserves in the crust (Jha et al. 2016; Prodius et al. 2020; Rademaker et al. 2013). Thus, the recovery of end-of-life products containing REEs (electronic equipment such as fluorescent lamps and NdFeB magnets, industrial wastes such as bauxite residue and coarse coal refuse) was listed as a crucial development strategy (Botelho Junior et al. 2021a, b; Kaya et al. 2021; Zhang and Honaker 2018). More than 20% of the REEs produced globally was used to produce NdFeB magnets, which were an indispensable part of many high-tech devices (Lixandru et al., 2017). At the same time, the REE content in NdFeB magnets was particularly high (up to 30%) (Moore et al. 2015; Önal et al. 2017), so the discarded NdFeB magnets have progressively become the focus of recycling materials.

Several processes have been proposed to recover REEs from NdFeB magnets, such as hydrometallurgical approaches (Jha et al. 2016), pyrometallurgical approaches

Responsible Editor: Ioannis A. Katsoyiannis

✉ Nengwu Zhu  
nwzhu@scut.edu.cn

- <sup>1</sup> School of Environment and Energy, South China University of Technology, Guangzhou 510006, People's Republic of China
- <sup>2</sup> The Key Laboratory of Pollution Control and Ecosystem Restoration in Industry Clusters Ministry of Education, Guangzhou 510006, People's Republic of China
- <sup>3</sup> Guangdong Provincial Key Laboratory of Solid Wastes Pollution Control and Recycling, Guangzhou 510006, People's Republic of China
- <sup>4</sup> Guangdong Environmental Protection Key Laboratory of Solid Waste Treatment and Recycling, Guangzhou 510006, People's Republic of China

(Bian et al. 2016; Hua et al. 2014), gas phase extraction (Mochizuki et al. 2013; Walton et al. 2015), ionic liquid extraction (Dupont and Binnemans 2015), and membrane solvent extraction (Kim et al. 2015), etc. Due to the advantages of large capacity, high REE recovery efficiency, and high purity of recycled products, hydrometallurgical approaches still aroused the interest of scholars. However, traditional hydrometallurgical route consumed a lot of acid and commonly produced a large amount of wastewater, which limited its development (Binnemans et al. 2013). Venkatesan et al. (2018a) reported that the NdFeB magnets were completely dissolved with HCl, Fe (II) was selectively oxidized to Fe (III) by in situ electrochemical oxidation, and rare earth ions were precipitated with oxalic acid. Furthermore, Venkatesan et al. (2018b) proposed a repeated electrolysis-dissolution-precipitation method to selectively recover 95% of REEs with the recovered products purity more than 99%. In the above process, the HCl was recycled, which could reduce secondary pollution. In addition, Kumari et al. (2018) recovered 98% of REEs by roasting NdFeB magnets and leaching the rare earth oxides (REOs) with HCl, and the oxalic acid precipitated product was calcined to obtain REOs with a purity of 99%.

Some researchers achieved environment-friendly recovery of resources by changing the type of leaching agents. At the same time, sample pretreatment is an important link in many processes, more attention should be paid to it. To our best knowledge, mechanical activation was a very popular pretreatment method, which had been studied in the field of secondary resource recovery, especially in the field of waste trichromatic phosphors treatment (Yuan et al. 2013; Ou and Li 2014; Tan et al. 2016). Pretreatment of trichromatic phosphors by mechanical activation method could reduce its stability and greatly improved the leaching efficiency of REEs than the conventional hydrometallurgical processes (Song et al. 2017; Tan and Li 2015). It implied that if a suitable pretreatment method is adopted, the properties of the material might be improved, which have a favorable effect on the recovery of REEs.

In this study, an effective strategy to recover REEs from discarded NdFeB magnets by ball milling activation coupled with selective leaching of hydrochloric acid was proposed. Firstly, discarded NdFeB magnets were fully oxidized by roasting and then activated by ball milling at different ball milling speeds. Subsequently, the activated REEs were selectively leached with HCl, and factors including acid concentration and solid-liquid ratio were explored respectively. After that, oxalic acid was used to selectively precipitate

REEs to generate rare earth oxalates. Finally, rare earth oxalates were converted into final products REOs by roasting.

## Materials and methods

### Materials

The NdFeB magnets used in this study were the same batch as those used in our previous study (Liu et al. 2019). Firstly, the magnets were heated up to 400 °C for 30 min under the argon stream (50 mL/min) to ensure both high than the Curie temperature and the purpose of demagnetization. After being cooled to the room temperature, the unwanted iron cover and organic residues on the surface could be easily removed. Then, the NdFeB magnets were crushed to the particle size < 150 μm with a grinder. As shown in Table 1, the main chemical compositions of the NdFeB powder are 69.03% of Fe, 13.55% of Nd, 7.63% of Gd, and 3.45% of Pr with other elements (such as La, Ce, Dy, Er, Al, Cu, Co, Ni, B) less than 1%. Before mechanical activation, NdFeB magnet powders were roasted in order to convert the components of NdFeB magnets into corresponding oxides. The specific method was to lay NdFeB magnet powder (thickness is less than 1 mm) in a corundum boat, and maintained for 120 min in a muffle furnace. The oxidation roasting temperature was determined by thermogravimetric curve.

### Methods

#### Mechanical activation of oxide magnets

The mechanical activation process was carried out in planetary mill (Retsch PM 100, RETSCH, Hahn, Dusseldorf, Germany). First of all, 8 g oxidized NdFeB magnet powders were placed in a 50-mL stainless steel ball grinding tank, and then 12 stainless steel balls with diameter of 10 mm were added. The ball mill was activated at 300, 500, and 650 rpm for 60 min. In order to prevent superheated powder from bonding, the samples were ground for 10 min at intervals of 10 min for 6 times. The activated samples were sealed for subsequent leaching experiments.

#### Leaching of activated magnets

The leaching experiment was carried out in a 100-mL flask, heated by a constant temperature water bath, and stirred by a magnetic stirrer. The effects of ball milling speed (revolution

**Table 1** Chemical composition of the NdFeB magnets

| Element | Fe    | Nd    | Gd   | Pr   | La   | Ce   | Dy   | Er   | Al   | Cu   | Co   | Ni   | B    |
|---------|-------|-------|------|------|------|------|------|------|------|------|------|------|------|
| Mass. % | 69.03 | 13.55 | 7.63 | 3.45 | 0.14 | 0.13 | 0.06 | 0.06 | 0.92 | 0.19 | 0.07 | 0.01 | 0.91 |

speed), hydrochloric acid concentration, and solid–liquid ratio on the leaching efficiency of REEs and iron were investigated. The leaching temperature was set to 90 °C, the stirring speed of magnetic stirrer was set to 500 rpm, and the leaching time was 180 min. In the process of leaching, 2 mL samples were taken regularly with syringe at 5, 10, 20, 30, 60, 90, 120, 150, and 180 min after the beginning of leaching, obtaining the leachate through a 0.22- $\mu\text{m}$  filter. The contents of REEs elements and iron were determined by inductively coupled plasma optical emission spectrometry (ICP-OES), and the leaching efficiency was calculated. The calculation method was consistent with that used by Song et al. (2017). After the leaching process, the sample was cooled naturally to room temperature and then filtered.

### Selective precipitation and roasting

REEs in the leaching solution were precipitated with 10 g/L oxalic acid solution to obtain rare earth oxalates. The dosage of oxalic acid was calculated according to the content of REEs in leaching solution. Rare earth oxalates were separated from the solution by suction and then vacuum freeze dried. Finally, the dried rare earth oxalates were laid flat in the corundum boat (the thickness is less than 1 mm), then heated to 800 °C in the muffle furnace for 120 min to obtain rare earth oxides.

### Characterization

The chemical composition of the samples was analyzed by ICP-OES (Agilent ICP 730, Agilent Technologies, Santa Clara, CA, USA). X-ray diffraction (Xpert pro M, Philips, Almelo, Netherlands) with Cu K $\alpha$  radiation was used to analyze the phase of powder samples. The morphology of the samples was observed by scanning electron microscopy (Merlin S-3700 N, ZEISS, Aalen, Baden-Württemberg, Germany) with energy-dispersive X-ray spectroscopy (Oxford X-Max, Oxford Instruments, Abingdon, Oxfordshire, England). Laser particle size analyzer (MS2000, Malvern Instruments, Malvern, England) was used to analyze the particle

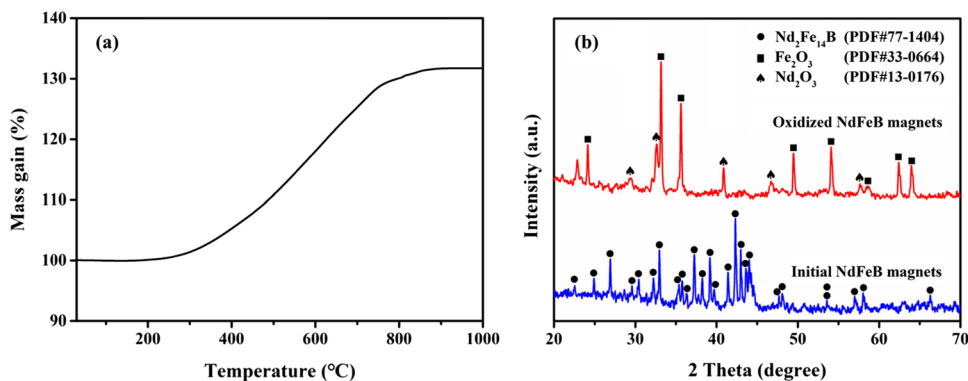
size of powder samples from 0.02 to 2000  $\mu\text{m}$ , and the dispersant used was ultra-pure water.

## Results and discussion

### Physicochemical properties change of samples after roasting

If the REEs in NdFeB magnets are leached directly with hydrochloric acid without oxidation roasting, a large amount of iron elements will be leached into the solution, so that the iron element needs to be removed by precipitation method. However, about 30% of the REEs was lost due to co-precipitation (Rabatho et al. 2013). Therefore, NdFeB magnets needed to be roasted before leaching experiments, so that the iron element in NdFeB magnets could be converted into stable  $\text{Fe}_2\text{O}_3$ . Compared with REOs,  $\text{Fe}_2\text{O}_3$  was less susceptible to corrosion by hydrochloric acid, so REEs could be selectively leached by controlling the concentration of hydrochloric acid (Jiang et al. 2013; Kumari et al. 2018). The minimum temperature required for absolute oxidation of the elements in the sample was obtained by thermogravimetric analysis. The thermogravimetric curves drawn from the analysis results were shown in Fig. 1a. It revealed that when the temperature was heated from room temperature to about 200 °C, the mass of the sample remained almost unchanged. Then, the sample began to gain weight continuously with the increase of temperature. When the temperature was about 900 °C, a weight-increasing platform region appeared. Thereafter, the mass of the sample remained unchanged with the increase of temperature, indicating that the sample had been absolutely oxidized. The theoretical weight gain of 32.93% was calculated for the conversion of all elements in the sample to the corresponding oxides. Thermogravimetric analysis showed that the actual weight gain of the sample was 32.50%, which was very close to the theoretical weight gain. It was also proved that the sample had been completely oxidized after roasting at 900 °C.

**Fig. 1** a TGA curve of discarded NdFeB magnets powder; b XRD pattern of NdFeB magnets powder before and after roasting



The samples before and after roasting were analyzed by X-ray diffraction (XRD). The results were shown in Fig. 1b. After roasting, the characteristic peaks of the  $\text{Nd}_2\text{Fe}_{14}\text{B}$  phase in the original NdFeB magnets disappeared, replaced by the characteristic peaks of the  $\text{Fe}_2\text{O}_3$  phase and the  $\text{Nd}_2\text{O}_3$  phase. Seven characteristic peaks ( $2\theta = 24.1^\circ, 33.1^\circ, 35.6^\circ, 49.4^\circ, 54.0^\circ, 62.5^\circ, 63.9^\circ$ ) of  $\text{Fe}_2\text{O}_3$  phase and five characteristic peaks ( $2\theta = 29.3^\circ, 31.3^\circ, 41.1^\circ, 46.1^\circ, \text{and } 58.0^\circ$ ) of  $\text{Nd}_2\text{O}_3$  phase could be clearly observed from the XRD pattern of NdFeB magnets, which indicated that NdFeB magnets had been completely converted into corresponding oxides by roasting at  $900^\circ\text{C}$  for 120 min. Therefore,  $900^\circ\text{C}$  was chosen as the roasting temperature of NdFeB magnets.

### Physicochemical properties change of samples after mechanical activation

After ball milling activation, the color of the sample changed from grayish brown to reddish brown. The particle size distribution of samples before and after activation at different milling speeds was shown in Fig. 2a. It was found that the particle size distribution of the sample without activation was between 0.2 and  $400\ \mu\text{m}$ , and the particle size of the sample after ball milling activation was less than  $100\ \mu\text{m}$ . With the increase of ball milling speed, the particle size of the sample decreased gradually. The main reason for the decrease of particle size was that the kinetic energy produced by the collision between the balls was transferred to the sample and transformed into the internal energy of the sample in the process of ball milling activation. With the increase of ball milling speed, the collision frequency between the balls increased, and the internal energy transferred to the sample increased, resulting in the decrease of the particle size of the sample.

The change of the particle size of the sample can cause the change of its specific surface area. The median particle size and the specific surface area were shown in Fig. 2b. It could be seen from the figure that the median particle size was  $24.303\ \mu\text{m}$  and the corresponding specific surface area was only  $0.54\ \text{m}^2/\text{g}$  when the sample was not activated.

After 300-rpm ball milling speed activation, the median particle size of the sample decreased sharply to  $4.416\ \mu\text{m}$ , but the specific surface area increased to  $4.32\ \text{m}^2/\text{g}$ . With the increase of ball milling speed, the median particle size and specific surface area of the sample still decreased, but the range of variation slowed down. When the ball milling speed was increased to 650 rpm, the median particle size of the sample was only  $1.535\ \mu\text{m}$ , while the corresponding specific surface area was increased to  $6.79\ \text{m}^2/\text{g}$ .

In the study of waste fluorescent lamp powder by Song et al. (2017) and Tan et al. (2016), the van der Waals force could significantly increase when the particle size decreased to a certain extent with the increase of ball milling speed, resulting in local plastic deformation and mutual penetration in the contact zone of adjacent particles. So, the fine particles could be agglomerated, leading to the increase of particle size and the decrease of specific surface area. In this study, with the increase of ball milling speed, the particle size of the sample had been decreasing and the specific surface area had been increasing. Even when the ball milling speed increased to 650 rpm, the trend had not changed. This indicated that the agglomeration of NdFeB magnet did not occur after 60-min activation at the ball milling speed designed by the present experiment, possibly due to the different structure of NdFeB magnets and fluorescent lamp powders. In fact, no agglomeration of the sample particles was more conducive to the subsequent leaching process.

The surface morphology of samples before and after activation at different milling speeds was observed by scanning electron microscopy (SEM). The results were shown in Fig. 3. It could be seen from Fig. 3a that before ball milling activation, the sample was consisted of many large particles with similar size and uniform distribution. The particle size was mostly around  $20\ \mu\text{m}$ , which corresponded to the highest peak of the particle size distribution curve in Fig. 2a. After 300-rpm ball milling speed activation, many fine particles could be clearly seen in the sample (Fig. 3b), which was mainly caused by friction, shear, impact, and collision during ball milling. However, there were still some relatively large particles in the samples activated by ball milling. The

**Fig. 2** a Particle size distribution; b specific surface area and medium particle size of samples activated at different ball milling speeds

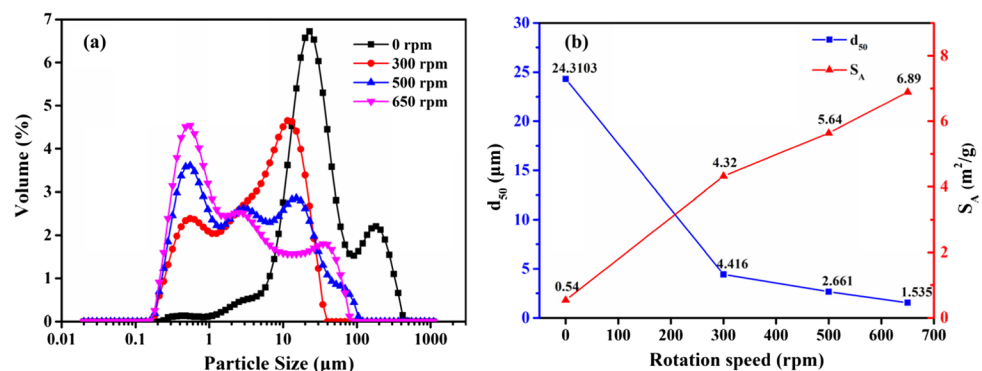


**Fig. 3** SEM images of samples activated at different ball milling speeds

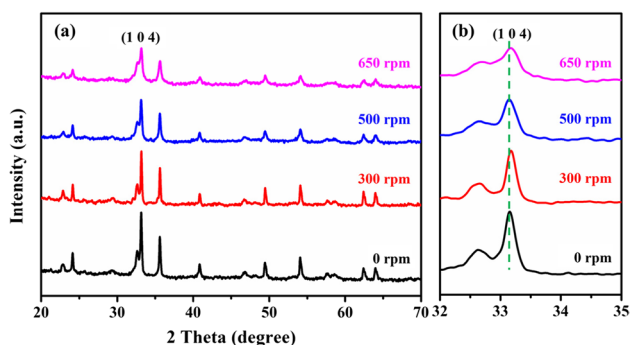
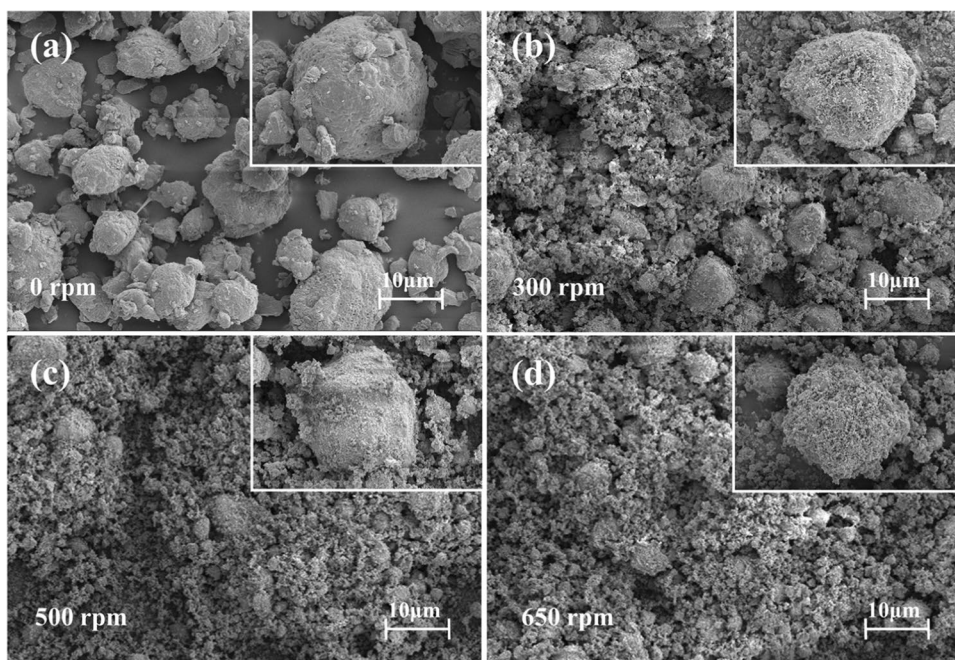


**Fig. 4** **a** XRD patterns of samples activated at different ball milling speeds and **b** partial enlarged image

particle size was about 10  $\mu\text{m}$ , which was also consistent with the highest peak of the corresponding curve of particle size distribution. As the ball milling speed increased, the damage of those effects on large particles increased, resulting in more fine particles. The difference between the two samples was very difficult to distinguish after 500-rpm and 650-rpm ball milling speed activation from Fig. 3c and d, which was very consistent with the results of the corresponding two curves in particle size distribution.

XRD pattern of the samples before and after activation at different ball milling speeds was shown in Fig. 4. The right side was an enlarged image of the spectra near  $2\theta = 33.381^\circ$ . The figure showed that no new phase was formed after the sample was activated by ball milling. However, with the increase of ball milling speed, the peak strength of the characteristic peak gradually decreased and the line width gradually

widened. This was the common feature of mechanical force on material structure change. In the process of ball milling activation, mechanical force and lattice defects changed the crystal structure of the sample, resulting in the deterioration of the crystallinity of the sample. The higher the ball milling speed was, the worse the crystallinity of the sample became. For the subsequent leaching process, the variation of crystallinity of samples was also beneficial to the leaching of REEs.

From the above discussion, it could be concluded that the effect of ball milling activation on the physicochemical properties of discarded NdFeB magnets was mainly manifested in two aspects. On the one hand, ball milling led to a decrease in the particle size of NdFeB magnets, which would contribute to the formation of new surfaces, thus increasing the specific surface area of the sample. On the other hand, ball milling brought about considerable deformation of the crystal structure of discarded NdFeB magnets, which resulted in the increase of lattice defects and local reactivity. Therefore, the changes of physicochemical properties of discarded NdFeB magnets caused by ball milling activation would be beneficial to the leaching of REEs by hydrochloric acid, thus improving the leaching efficiency and leaching speed of REEs.

## Leaching behavior changes of REEs from samples after mechanical activation

### The effect of ball milling activation

In the process of selective leaching with hydrochloric acid, the effect of different milling speeds on the leaching

efficiency of REEs in discarded NdFeB magnets was studied at first. Four levels of 0, 300, 500, and 650 rpm were set up, of which 0 rpm was the control group without ball milling activation. The concentration of hydrochloric acid used was 0.8 M and the solid–liquid ratio was 60 g/L. Figure 5 showed that the leaching efficiency of REEs increased gradually with the prolongation of leaching time for the sample without mechanical activation. After 180 min of leaching, the leaching efficiency of REEs reached the maximum (about 98%). After ball milling activation, the leaching efficiency of REEs also increased with the extension of leaching time. However, unlike the unactivated samples, the leaching efficiency of REEs in the activated samples reached more than 99%, and the leaching speed of REEs increased obviously with the increase of ball milling speed. When the ball milling speed was 300 rpm, the leaching efficiency of REEs reached more than 99% after 150 min. When the speed was increased to 500 rpm, the time required to achieve the same efficiency (more than 99%) was shortened to 120 min. And when the speed continued to increase to 650 rpm, the time required was only 60 min. The results showed that ball milling activation can strengthen the leaching of REEs and improve the leaching efficiency and leaching speed of REEs. The higher the ball milling speed, the higher the leaching speed of REEs becomes. This was in line with the results obtained by Tan et al. (2016) and Song et al. (2017) in leaching REEs from waste fluorescent lamp powder.

At the same time, it was found that with the increase of ball milling speed, the leaching efficiency of iron as impurity also increased. According to the data shown in Fig. 5, when the sample was not activated, the leaching efficiency of iron only reached 10.1%. After 300-, 500-, and 650-rpm ball milling speed activation, the maximum leaching efficiency of iron reached 13.4%, 14.6%, and 19.3% respectively.

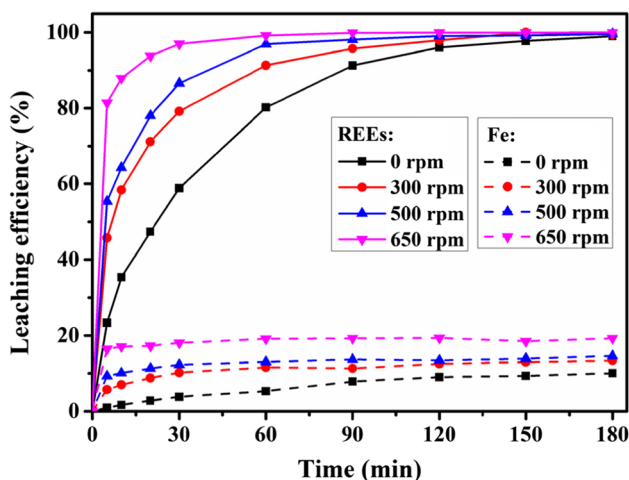


**Fig. 5** The effect of ball milling speed on leaching efficiency of REEs and iron

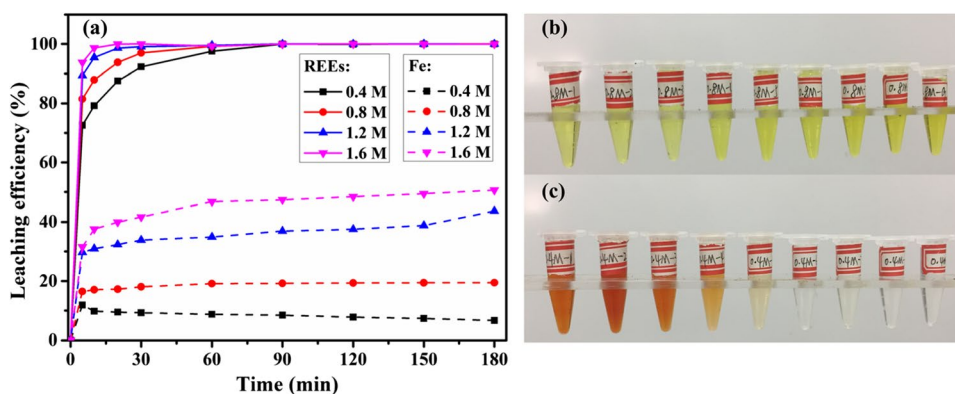
Compared with the unactivated samples, the leaching efficiency of iron was increased by about twice when the ball milling speed reached the maximum speed of 650 rpm. This indicated that the ball milling activation method promoted the leaching of impurity iron elements as well as the leaching of REEs. However, in order to make the leaching effect of REEs the best, 650 rpm was chosen as the best ball milling speed in the next experiment. As for the leaching of impurity iron, we regulated other leaching conditions, so as to reduce the impact of leaching on the recovery of REEs.

### The effects of hydrochloric acid concentration

A total of 0.4, 0.8, 1.2, and 1.6 M gradients of hydrochloric acid were set up in this group of experiments. The ball milling speed of sample pretreatment was set to 650 rpm and the solid–liquid ratio was set to 60 g/L. The results were shown in Fig. 6a. It could be seen from the figure that with the prolongation of leaching time, the leaching efficiency of REEs reached more than 99% under different hydrochloric acid concentration, and the leaching speed of REEs increased with the increase of hydrochloric acid concentration. When the concentration of hydrochloric acid was 0.4 M, the leaching efficiency of REEs reached more than 99% after leaching for 90 min. With the increase of hydrochloric acid concentration, the time required for REEs leaching efficiency to reach this level was gradually shortened. When hydrochloric acid concentration increased to 1.6 M, this time only took 20 min. Furthermore, in addition to the 0.4 M concentration of hydrochloric acid, the leaching efficiency of iron element gradually increased as the concentration of hydrochloric acid increased. Especially when the concentration of hydrochloric acid was increased to 1.2 M and 1.6 M, the maximum leaching efficiency of iron could be as high as 43.7% and 50.6%. Obviously, the purpose of selective leaching of REEs from NdFeB magnets might not be achieved. The leaching of large amounts of iron element seriously affected the subsequent recovery process of REEs.

However, when the concentration of hydrochloric acid was 0.4 M, the leaching efficiency of REEs reached 99% only after 90 min, while the leaching efficiency of impurity iron was very low. Moreover, the trend of leaching efficiency of iron was different when using other concentrations. Although the leaching efficiency of iron increased to 11.8% after 5 min, it began to decline slowly and dropped to 6.7% after 180 min. This indicated that the concentration of iron ion in solution increased gradually in the initial stage of leaching, and then decreased with the extension of leaching time. Kumari et al. (2018) also found this phenomenon in the experiment of studying the effect of hydrochloric acid concentration on the leaching efficiency of REEs in NdFeB magnets. This was because when the concentration of hydrochloric acid was 0.4 M, the concentration of hydrogen ion

**Fig. 6** a The effect of HCl concentration on leaching efficiency of REEs and iron; sample photos taken at regular intervals under leaching at HCl concentrations of b 0.8 M and c 0.4 M



was very low. With the leaching reaction proceeding, the hydrogen ion was gradually consumed, the solution pH gradually increased, and the critical pH value of iron ion hydrolysis was gradually reached. Thus, iron ions dissolved in the initial stage of leaching began to hydrolyze to form Fe(OH)<sub>3</sub>, which resulted in a gradual decrease in the concentration of iron ions in the solution.

This was also confirmed by the phenomena observed during regular sampling with syringes. When the concentration of hydrochloric acid was 0.8, 1.2, and 1.6 M, the leachate of the sample filtered by the syringe was yellow brown (Fig. 6b), which was the color of typical FeCl<sub>3</sub> solution. However, when the concentration of hydrochloric acid was 0.4 M, the sample showed reddish brown instead of yellow brown after filtration, and the color became lighter and lighter with the prolongation of leaching time (Fig. 6c). This was because the leaching efficiency of iron at 0.4 M hydrochloric acid concentration was relatively low and FeCl<sub>3</sub> generated was very small, so it was difficult to show brown. The hydrolysis of iron ions was a reversible reaction. The red-brown Fe(OH)<sub>3</sub> colloid formed in the initial stage of the reaction could not precipitate due to the reaction equilibrium. In this experiment, with the leaching reaction proceeding, the hydrogen ions produced by hydrolysis of iron ions could be conducive to the leaching of REEs in the sample. As a result, the hydrolysis equilibrium was broken and Fe(OH)<sub>3</sub> was gradually precipitated, so the samples taken later became reddish brown and nearly transparent.

For this study, when the concentration of hydrochloric acid was 0.4 M, Fe(OH)<sub>3</sub> produced by hydrolysis of iron ions could eventually precipitate in the leaching residue, thus reducing the concentration of impurity iron ions in the leaching solution, which was actually beneficial to our REEs recovery process. However, when the concentration of hydrochloric acid was 0.8, 1.2, and 1.6 M, excessive hydrochloric acid would lead to the leaching of large amounts of iron elements, and those iron elements existed in the presence of iron ions in solution. At the same time, because of the high concentration of hydrogen ions and the low pH of

the solution, these iron ions could not hydrolyze and precipitate, thus affecting the subsequent recovery of REEs. In addition, using higher concentration of hydrochloric acid meant consuming more hydrochloric acid in the whole recovery process, thus causing higher economic costs and more waste acid for subsequent treatment, which was not conducive to our recovery process. So, the use of low concentration hydrochloric acid could not only be conducive to the selective leaching process of REEs, but also save economic cost and reduce environmental pollution. Therefore, hydrochloric acid with concentration of 0.4 M was used in the follow-up experiment.

#### The effects of solid–liquid ratio on REE leaching efficiency

Solid–liquid ratio also affected the leaching effect of REEs in samples. Four gradients of solid–liquid ratio were set up in this experiment, namely 40, 60, 80, and 100 g/L. The ball milling speed of sample pretreatment was 650 rpm and the concentration of hydrochloric acid was 0.4 M. It could be seen from Fig. 7 that the leaching efficiency of REEs reached more than 99% with the extension of leaching time under the four solid–liquid ratio gradients. The leaching speed of REEs decreased with the increase of solid–liquid ratio, which was different from the variation of ball milling speed and hydrochloric acid concentration. When the solid–liquid ratio was 40 g/L, more than 99% of REEs in the sample could be leached into the solution by hydrochloric acid within 60 min. With the increase of solid–liquid ratio, the time required for the leaching efficiency of REEs to reach this level was gradually prolonged. When the solid–liquid ratio increased to 100 g/L, it took 120 min to leach more than 99% of the REEs in the sample. Therefore, with the same volume of hydrochloric acid, the leaching efficiency of REEs decreased as the amount of sample added to it increased (i.e., the solid–liquid ratio increased). This conformed to the natural law of the general leaching reaction. The amount of treated sample increased, and the time required increased. However, the leaching efficiency of

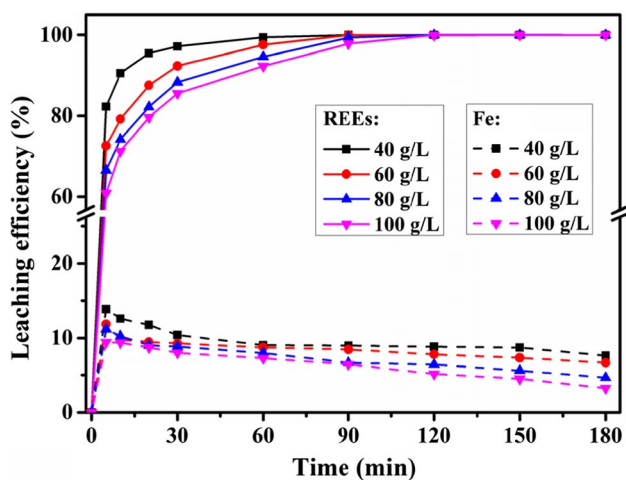


**Fig. 7** The effect of solid–liquid ratio on leaching efficiency of REEs and iron

REEs eventually reached more than 99%, which indicated that increasing the solid–liquid ratio meant making full use of hydrochloric acid, which could greatly save the amount of hydrochloric acid used in the whole recovery process. For example, when the solid–liquid ratio was 100 g/L, it took twice the time to attach the maximum leaching efficiency (more than 99%) compared with the solid–liquid ratio was 40 g/L, but the amount of sample treated by the former was 2.5 times than that of the latter. Therefore, increasing the solid–liquid ratio could reduce the hourly consumption of hydrochloric acid, which was economical and environment-friendly. Of course, the solid–liquid ratio also had an upper limit. When the amount of sample added exceeded the treatment capacity of hydrochloric acid, the REEs in the excess sample would no longer be leached, resulting in a decrease of the leaching efficiency of REEs. After theoretical calculation, we found that under the scale of current experimental design, the REEs in 10.3 g samples activated by ball milling could be completely leached with 0.4 M hydrochloric acid, i.e., the upper limit of solid–liquid ratio was 103 g/L. The

maximum solid–liquid ratio set in this study was 100 g/L, which was just a little lower than the upper limit. That was to say, the amount of hydrochloric acid used in the leaching process was slightly over the theoretical value. Therefore, 100 g/L was chosen as the best solid–liquid ratio for REEs leaching.

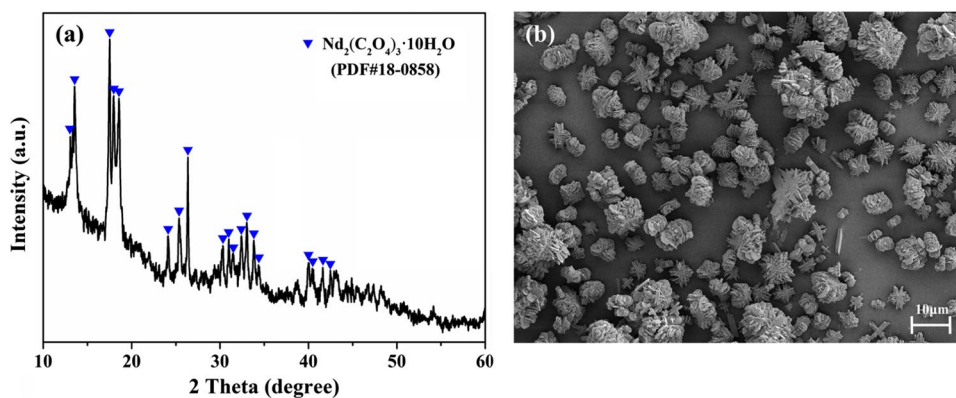
In addition, at the concentration of 0.4 M hydrochloric acid, the leaching efficiency of iron in samples with different solid–liquid ratios increased within the first 5 min, and then decreased gradually. Moreover, when the solid–liquid ratio increased from 40 to 100 g/L, the final leaching efficiency of iron decreased from 7.6 to 3.2%. Therefore, with the increase of solid–liquid ratio, the concentration of iron ion in leaching solution decreased, which was more conducive to the recovery of REEs. Therefore, 100 g/L could be used as the best solid–liquid ratio in the selective leaching process of hydrochloric acid.

### Characterization of REE oxalates and REE oxides

Based on the above results, we chose the leaching solution obtained under the conditions of ball milling speed 650 rpm, hydrochloric acid concentration 0.4 M, and solid–liquid ratio 100 g/L for the subsequent REE recovery process. After adding oxalic acid solution to the leaching solution, REEs precipitated in the form of rare earth oxalate, while other impurity metals remained in the leaching solution. XRD analysis (Fig. 8a) showed that the rare earth oxalate was  $\text{Nd}_2(\text{C}_2\text{O}_4)_3 \cdot 10\text{H}_2\text{O}$ , indicating that the hydrated oxalate of rare earth was formed. The surface morphology of rare earth oxalate hydrate was observed by SEM (Fig. 8b). It could be seen that rare earth oxalate hydrate was a kind of granule formed by stacking and crossing of lamellar crystals, and its particle size was in the range of 5–20  $\mu\text{m}$ . This characteristic was very similar to that of rare earth oxalates obtained by hydrochloric acid selective leaching of samples without ball milling activation by Kumari et al. (Kumari et al. 2018).

There were four strong characteristic peaks of REOs at the positions of  $2\theta = 27.857^\circ$ ,  $32.267^\circ$ ,  $46.308^\circ$ , and  $54.935^\circ$ ,

**Fig. 8** a XRD and b SEM images of rare earth oxalates obtained by precipitation





corresponding to (222), (400), (440), and (622) crystal planes of  $\text{Nd}_2\text{O}_3$  phase, respectively (Fig. 9a). This indicated that REOs were indeed formed after roasting of rare earth oxalate hydrate.

The surface morphology of the obtained REOs was observed by SEM. It could be seen from Fig. 9b that most of the REEs were also particles formed by stacking and crossing of lamellar crystals with a diameter of about 10  $\mu\text{m}$ . Unlike the experimental results of Kumari et al. (2018), the REOs obtained in this study contained a small number of particles formed by cross-section of columnar crystals. In addition, EDS was used to analyze the obtained REOs, of which only three main rare earth elements were scanned. Figure 9c showed that the contents of Nd, Gd, Pr, and O in REEs were very high, while the contents of Fe were very low, which indicated that the purity of recovered REEs was high. The purity of recovered REOs reached 99.9% by ICP-OES analysis.

## Implications

The hydrometallurgical process had a great advantage in the recovery of rare earth metals from discarded NdFeB magnets due to the availability of a single REO with a wider range of applications (Tuncuk et al. 2012). In addition, the mixed REOs obtained by pyrometallurgical process

would eventually have to be separated by hydrometallurgical process to obtain a single REO. However, the cost and secondary pollution of hydrometallurgical process due to the consumption of a large number of inorganic acids and extractants could not be ignored (Jyothi et al. 2020; Xu et al. 2004). Therefore, in the case of giving full play to the advantages of hydrometallurgical process, it was particularly important to improve its shortcomings. In this study, ball milling activation method was used to pretreat samples before hydrochloric acid selective leaching process. Compared with the samples without ball milling activation, the physical properties of samples changed greatly, which was beneficial to the subsequent leaching of REEs in the process of selective leaching of hydrochloric acid. Therefore, the hydrometallurgical process of NdFeB magnets was successfully improved and innovated by ball milling activation method, and the leaching effect of REEs was improved. The comparison of different process for recovery of rare earths from NdFeB magnet is given in Table 2. It showed that the REE recovery efficiency and recovered REO purity of mechanical activation coupled with acid leaching process are quite good than other process, which indicated that the proposed strategy has an excellent effect for the recovery of REEs from discarded NdFeB magnets.

At present, for the recovery of secondary rare earth metals, non-salt ball milling activation was not been reported

**Fig. 9** a XRD, b SEM, and c EDS images of the obtained REOs

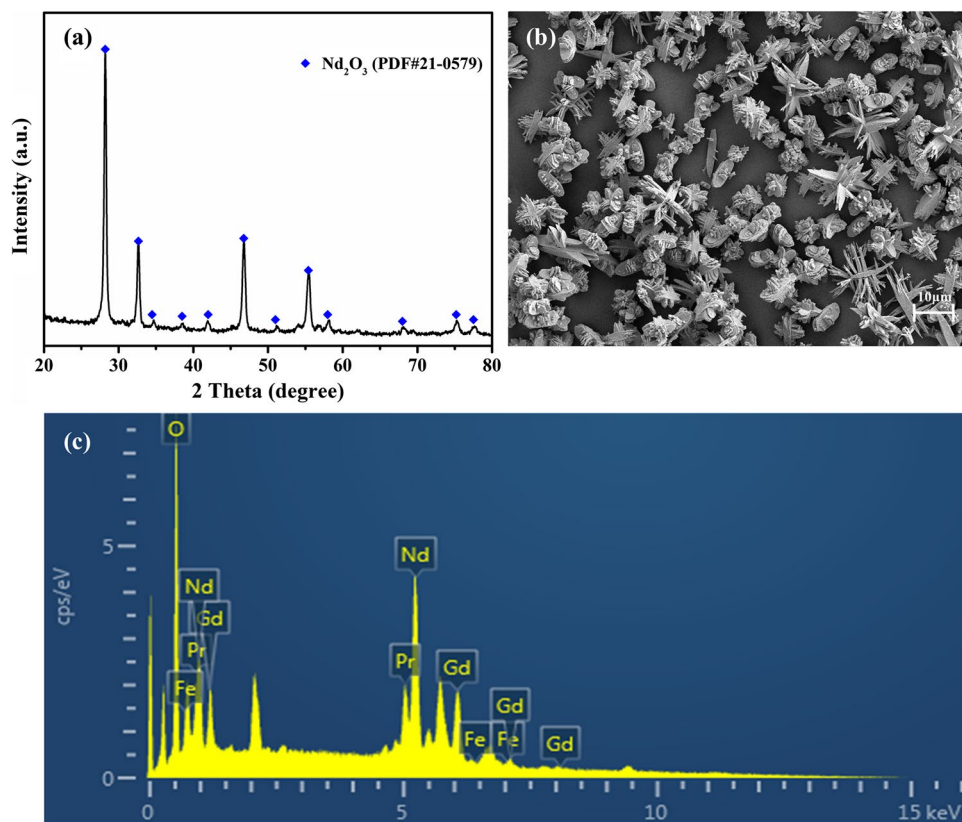


**Table 2** The comparison of different process for recovery of rare earths from NdFeB magnet

| Process  | Reaction conditions   | Efficiency   | References           |
|--|---|--|----------------------|
| Sulfation roasting followed by leaching          | Roasting at 750°C for 1 h, leaching at 25°C for 1 h   | REE recovery efficiency $\geq$ 95%<br>REO purity > 98%                     | (Önal et al. 2015)   |
| Leaching and selective precipitation             | 6 mol/L hydrochloric acid, 50 g/L tartaric acid, 313 K  | REE leaching 99.27%<br>REE recovery efficiency 90.18%<br>REO purity 95.83% | (Tian et al. 2019)   |
| Chlorination roasting and water leaching         | Roasting at 300°C for 3 h with 3 times stoichiometric amount of $\text{NH}_4\text{Cl}$ , leaching at 95°C for 1 h with 100 g/L pulp density | REE recovery efficiency 98%<br>REO purity 99.2%                            | (Kumari et al. 2021) |
| Mechanical activation coupled with acid leaching | 650-rpm ball milling speed, 0.4 M hydrochloric acid, and 100 g/L solid–liquid ratio   | REE recovery efficiency > 99%<br>REO purity 99.9%                          | This study           |

in the field of discarded NdFeB magnets, but there were some studies in the field of waste fluorescent lamp powder treatment. From the perspective of rare earth leaching efficiency, compared with the leaching of rare earth in waste fluorescent lamp powder, the leaching efficiency of REEs in discarded NdFeB magnets seemed to increase slightly from 98 to 99% without and with ball milling activation. This was because REEs such as neodymium, gadolinium, praseodymium, and dysprosium in NdFeB magnets were easier to leach than those of yttrium, europium, cerium, and terbium in waste fluorescent lamp powders (Tan et al. 2016). Therefore, when ball milling activation method was used to strengthen the leaching efficiency, the growth space was smaller. But when the leaching efficiency reached 98%, it was a great progress to raise another percentage point. From the perspective of the leaching speed of REEs, the speed increased significantly when ball milling activation method was applied to discarded NdFeB magnets. When the ball milling speed reached the maximum speed of experiment design, the leaching speed of REEs increased about 3 times. The increase of REE leaching speed will greatly shorten the time required for the whole recovery process and improve the recovery efficiency. Compared with the leaching of NdFeB magnets without ball milling activation by Kumari et al. (2018), the leaching efficiency of iron after activation in this study was higher, which indicated that ball milling activation can also promote the leaching of iron. However, subsequent studies found that the selective leaching of REEs could be achieved by controlling the concentration of hydrochloric acid and the solid–liquid ratio. Therefore, on the basis of enhancing the leaching effect, the proposed strategy could shorten the leaching time and reduce the acid consumption.

In the future, the activation and leaching conditions can be controlled more finely in order to further improve the leaching efficiency of REEs and reduce the leaching efficiency of iron element. In the other application of ball milling activation methods, the co-grinding of doped

sulfur (Yuan et al. 2013; Ou and Li 2014), iron (Zhang et al. 2016), and  $\text{Al}_2\text{O}_3$  (Zhang et al. 2000) particles achieved satisfactory recovery results. Therefore, it can be considered to dope NdFeB magnets with other material particles to co-grind to save time and simplify the process, or to react with iron elements to form stable compounds, which the resulting compounds are a product with higher application value than iron oxide. In addition, some scholars have initially studied the use of mechanical activation coupled with leaching process to recover valuable metals (Fan et al. 2018; Fathy et al. 2021), which indicates that the proposed strategy may be used for different types of e-waste.

## Conclusion

Ball milling activation method effectively improved the leaching efficiency and leaching speed of REEs in discarded NdFeB magnets during selective acid leaching. After ball milling activation, the leaching efficiency of REEs increased to more than 99%. Under the optimum activation speed of 650 rpm, the leaching speed of REEs was three times higher than that of without activation. Reducing the concentration of hydrochloric acid and increasing the solid–liquid ratio were beneficial to reducing the leaching of iron and making full use of hydrochloric acid, thus reducing the consumption of hydrochloric acid and saving economic costs. The final purity of recovered REOs reached up to 99.9% under the conditions of 650-rpm ball milling speed, 0.4 M hydrochloric acid, and 100 g/L solid–liquid ratio. The combination of ball milling activation and selective acid leaching could be a favorable method in the treatment of discarded NdFeB magnets, which not only realized the efficient recovery of REEs, but also reduced the acid consumption and leaching time of the whole hydrochloric acid selective leaching process.

**Author contribution** Fulin Mao: conceptualization, methodology, writing—original draft, investigation, writing—review & editing. Nengwu Zhu: conceptualization, supervision, validation. Wen Zhu: data curation, resources. Bowen Liu: writing—review & editing. Pingxiao Wu: writing—review & editing. Zhi Dang: writing—review & editing.

**Funding** This study was financially supported by the National Key Research and Development Project (2019YFC1906900) and the Guangdong Science and Technology Project (2020B121201003 and 2017A020216013).

**Data availability** All data generated or analyzed during this study are included in this published article.

## Declarations

**Ethics approval and consent to participate** This manuscript does not involve human participants, human, data, or human tissue.

**Consent for publication** The manuscript does not contain any individual person's data.

**Conflict of interest** The authors declare no competing interests.

## References

- Bian Y, Guo S, Jiang L, Liu J, Tang K, Ding W (2016) Recovery of rare earth elements from NdFeB magnet by VIM-HMS method. *ACS Sustain Chem Eng* 4:810–818. <https://doi.org/10.1021/acssuschemeng.5b00852>
- Binnemans K, Jones PT, Blanpain B, Gerven TV, Yang Y, Walton A, Buchert M (2013) Recycling of rare earths: a critical review. *J Clean Prod* 51:1–22. <https://doi.org/10.1016/j.jclepro.2012.12.037>
- Botelho Junior AB, Espinosa DCR, Tenório JAS (2021a) Characterization of bauxite residue from a press filter system: comparative study and challenges for scandium extraction. *Min Metall Explor* 38:161–176. <https://doi.org/10.1007/s42461-020-00333-3>
- Botelho Junior AB, Espinosa DCR, Tenório JAS (2021b) The use of computational thermodynamic for yttrium recovery from rare earth elements-bearing residue. *J Rare Earths* 39:201–207. <https://doi.org/10.1016/j.jre.2020.02.019>
- Dupont D, Binnemans K (2015) Recycling of rare earths from NdFeB magnets using a combined leaching/extraction system based on the acidity and thermomorphism of the ionic liquid [Hbet][Tf<sub>2</sub>N]. *Green Chem* 17:2150–2163. <https://doi.org/10.1039/c5gc00155b>
- Fan E, Li L, Zhang X, Bian Y, Xue Q, Wu J, Wu F, Chen R (2018) Selective recovery of Li and Fe from spent lithium-ion batteries by an environmentally friendly mechanochemical approach. *ACS Sustain Chem Eng* 6:11029–11035. <https://doi.org/10.1021/acssuschemeng.8b02503>
- Fathy MA, Abdelbasir SM, Hassan SS, Kamel AH, Rayan D (2021) Mechanochemical activation for lead extraction from spent cathode ray tube. *J Mater Cycles Waste Manag* 23:1090–1101. <https://doi.org/10.1007/s10163-021-01198-4>
- Firdaus M, Rhamdhani MA, Rankin WJ, Pownceby M, Webster NAS, D'Angelo AM, McGregor K (2018) High temperature oxidation of rare earth permanent magnets. Part 1 – Microstructure evolution and general mechanism. *Corros Sci* 133:374–385. <https://doi.org/10.1016/j.corsci.2018.01.040>
- Hua Z, Wang J, Wang L, Zhao Z, Li X, Xiao Y, Yang Y (2014) Selective extraction of rare earth elements from ndfeb scrap by molten chlorides. *ACS Sustain Chem Eng* 2:2536–2543. <https://doi.org/10.1021/sc5004456>
- Jha MK, Kumari A, Panda R, Kumar JR, Yoo K, Lee JY (2016) Review on hydrometallurgical recovery of rare earth metals. *Hydrometallurgy* 165:2–26. <https://doi.org/10.1016/j.hydromet.2016.01.035>
- Jiang T, Zhang Y, Huang ZC, Li GH, Fan XH (2013) Preheating and roasting characteristics of hematite-magnetite (H-M) concentrate pellets. *Ironmak Steelmak* 35:21–26. <https://doi.org/10.1179/174328107X174771>
- Jyothi RK, Thenepalli T, Ahn JW, Parhi PK, Chung KW, Lee JY (2020) Review of rare earth elements recovery from secondary resources for clean energy technologies: Grand opportunities to create wealth from waste. *J Clean Prod* 267:122048. <https://doi.org/10.1016/j.jclepro.2020.122048>
- Kaya EE, Kaya O, Stopic S, Gürmen S, Friedrich B (2021) NdFeB magnets recycling process: an alternative method to produce mixed rare earth oxide from scrap NdFeB magnets. *Metals* 11. <https://doi.org/10.3390/met11050716>
- Kim D, Powell LE, Delmau LH, Peterson ES, Herchenroeder J, Bhavre RR (2015) Selective extraction of rare earth elements from permanent magnet scraps with membrane solvent extraction. *Environ Sci Technol* 49:9452–9459. <https://doi.org/10.1021/acs.est.5b01306>
- Kumari A, Sinha MK, Pramanik S, Sahu SK (2018) Recovery of rare earths from spent NdFeB magnets of wind turbine: leaching and kinetic aspects. *Waste Manag*. <https://doi.org/10.1016/j.wasman.2018.01.033>
- Kumari A, Raj R, Randhawa NS, Sahu SK (2021) Energy efficient process for recovery of rare earths from spent NdFeB magnet by chlorination roasting and water leaching. *Hydrometallurgy* 201:105581. <https://doi.org/10.1016/j.hydromet.2021.105581>
- Liu B, Zhu N, Li Y, Wu P, Dang Z, Ke Y (2019) Efficient recovery of rare earth elements from discarded NdFeB magnets. *Process Saf Environ Prot* 124:317–325. <https://doi.org/10.1016/j.psep.2019.01.026>
- Lixandru A, Venkatesan P, Jönsson C, Poenaru I, Hall B, Yang Y, Walton A, Güth K, Gauß R, Gutfleisch O (2017) Identification and recovery of rare-earth permanent magnets from waste electrical and electronic equipment. *Waste Manag* 68:482–489. <https://doi.org/10.1016/j.wasman.2017.07.028>
- Mochizuki Y, Tsubouchi N, Sugawara K (2013) Selective recovery of rare earth elements from Dy containing NdFeB magnets by chlorination. *ACS Sustain Chem Eng* 1:655–662. <https://doi.org/10.1021/sc4000187>
- Moore M, Gebert A, Stoica M, Uhlemann M, Löser W (2015) A route for recycling Nd from Nd-Fe-B magnets using Cu melts. *J Alloys Compd* 647:997–1006. <https://doi.org/10.1016/j.jallcom.2015.05.238>
- Önal MAR, Aktan E, Borra CR, Blanpain B, Gerven TV, Guo M (2017) Recycling of NdFeB magnets using nitration, calcination and water leaching for REE recovery. *Hydrometallurgy* 167:115–123. <https://doi.org/10.1016/j.hydromet.2016.11.006>
- Önal MAR, Borra CR, Guo M, Blanpain B, Gerven TV (2015) Recycling of NdFeB magnets using sulfation, selective roasting, and water leaching. *J Sustain Metall* 1:199–215. <https://doi.org/10.1007/s40831-015-0021-9>
- Ou Z, Li J (2014) Synergism of mechanical activation and sulfurization to recover copper from waste printed circuit boards. *RSC Adv* 4:51970–51976. <https://doi.org/10.1039/c4ra08265f>
- Prodius D, Gandha K, Mudring AV, Nlebedim IC (2020) Sustainable urban mining of critical elements from magnet and electronic wastes. *ACS Sustain Chem Eng* 8:1455–1463. <https://doi.org/10.1021/acssuschemeng.9b05741>
- Rabatho JP, Tongamp W, Takasaki Y, Haga K, Shibayama A (2013) Recovery of Nd and Dy from rare earth magnetic waste sludge

- by hydrometallurgical process. *J Mater Cycles Waste Manage* 15:171–178. <https://doi.org/10.1007/s10163-012-0105-6>
- Rademaker JH, Kleijn R, Yang Y (2013) Recycling as a strategy against rare earth element criticality: a systemic evaluation of the potential yield of NdFeB magnet recycling. *Environ Sci Technol* 47:10129–10136. <https://doi.org/10.1021/es305007w>
- Song G, Yuan W, Zhu X, Wang X, Zhang C, Li J, Bai J, Wang J (2017) Improvement in rare earth element recovery from waste trichromatic phosphors by mechanical activation. *J Clean Prod* 151:361–370. <https://doi.org/10.1016/j.jclepro.2017.03.086>
- Tan Q, Deng C, Li J (2016) Innovative application of mechanical activation for rare earth elements recovering: process optimization and mechanism exploration. *Sci Rep* 6:19961. <https://doi.org/10.1038/srep19961>
- Tan Q, Li J (2015) Recycling metals from wastes: a novel application of mechanochemistry. *Environ Sci Technol* 49:5849–5861. <https://doi.org/10.1021/es506016w>
- Tian Y, Liu Z, Zhang G (2019) Recovering REEs from NdFeB wastes with high purity and efficiency by leaching and selective precipitation process with modified agents. *J Rare Earth* 37:205–210. <https://doi.org/10.1016/j.jre.2018.10.002>
- Tuncuk A, Stazi V, Akcil A, Yazici EY, Deveci H (2012) Aqueous metal recovery techniques from e-scrap: hydrometallurgy in recycling. *Miner Eng* 25:28–37. <https://doi.org/10.1016/j.mineng.2011.09.019>
- Venkatesan P, Sun ZHI, Sietsma J, Yang Y (2018a) An environmentally friendly electro-oxidative approach to recover valuable elements from NdFeB magnet waste. *Sep Purif Technol* 191:384–391. <https://doi.org/10.1016/j.seppur.2017.09.053>
- Venkatesan P, Hoogerstraete TV, Hennebel T, Binnemans K, Sietsma J, Yang Y (2018b) Selective electrochemical extraction of REEs from NdFeB magnet waste at room temperature. *Green Chem* 20:1065–1073. <https://doi.org/10.1039/c7gc03296j>
- Walton A, Yi H, Rowson NA, Speight JD, Mann VSJ, Sheridan RS, Bradshaw A, Harris IR, Williams AJ (2015) The use of hydrogen to separate and recycle neodymium–iron–boron-type magnets from electronic waste. *J Clean Prod* 104:236–241. <https://doi.org/10.1016/j.jclepro.2015.05.033>
- Xu T, Li M, Zhang C (2004) Reclamation of Nd, Dy and Co oxides from NdFeB scrap. *Chin Rare Earths* 25:31–34. <https://doi.org/10.1117/12.528072>
- Yang Y, Walton A, Sheridan R, Güth K, Gauß R, Gutfleisch O, Buchert M, Steenari BM, Gerven TV, Jones PT, Binnemans K (2017) REE recovery from end-of-life NdFeB permanent magnet scrap: a critical review. *J Sustain Metall* 3:122–149. <https://doi.org/10.1007/s40831-016-0090-4>
- Yuan W, Li J, Zhang Q, Saito F, Yang B (2013) A novel process utilizing mechanochemical sulfidization to remove lead from cathode ray tube funnel glass. *J Air Waste Manage Assoc* 63:418–423. <https://doi.org/10.1080/10962247.2012.701194>
- Zhang W, Honaker RQ (2018) Rare earth elements recovery using staged precipitation from a leachate generated from coarse coal refuse. *Int J Coal Geol* 195:189–199. <https://doi.org/10.1016/j.coal.2018.06.008>
- Zhang Q, Lu J, Saito F, Nagata C, Ito Y (2000) Room temperature acid extraction of Co from  $\text{LiCo}_{0.2}\text{Ni}_{0.8}\text{O}_2$  scrap by a mechanochemical treatment. *Adv Powder Technol* 11:353–359. <https://doi.org/10.1163/156855200750172222>
- Zhang C, Zhuang L, Yuan W, Wang J, Bai J (2016) Extraction of lead from spent leaded glass in alkaline solution by mechanochemical reduction. *Hydrometallurgy* 165:312–317. <https://doi.org/10.1016/j.hydromet.2016.01.017>

**Publisher's note** Springer Nature remains neutral with regard to jurisdictional claims in published maps and institutional affiliations.